TPIV
Inference of the radial and poloidal velocity of the blobs in scrape-off layer from Gas Puff Imaging

Antoine Maier (antoine.maier@epfl.ch)

Supervisors:
Prof. Paolo Ricci (paolo.ricci@epfl.ch)
Davide Mancini (davide.mancini@epfl.ch)

January 9, 2022

1 Introduction

The world is facing today some global-scale issues, and one the most oppressing is the production of green energy. One good candidate for this is the thermonuclear fusion, that aims to fusion two light atomic nuclei into a heavier nucleus, in a reaction that produces energy. The advantage of this reaction is that it is green, in the sense that it does not produce carbon, contrary to the fossil fuels, such as coal, petroleum and natural gas. The electricity production by thermonuclear fusion is a challenge not already achieved by the humanity and scientists are still investigating some ways to achieve it. As of 2021, the leading fusion reactor is the Tokamak, and in particular the megaproject ITER which aims to achieve breakeven. Apart from ITER's tokamak, there are other tokamaks built in different countries that study various parameters. One of these smaller tokamaks is the Tokamak à configuration variable (TCV) located at École Polytechnique Fédérale de Lausanne (EPFL). This Tokamak investigates the shape of the plasma and its link with the performance of the fusion reactor.

To study plasma physics phenomena, scientists can design some experiments on a real tokamak but can also perform numerical simulations. One advantage with numerical simulations is the fact that we can directly observe the properties of interest at any considered region in the tokamak, whereas experimental research on a real device needs some ways to observe these quantities because they are not always accessible directly. However, the simulation of plasma in a tokamak device is computationally hungry and needs efforts to analyse the results extracted from it. The computational complexity of the simulation of a plasma in a tokamak device requires to simplify its equations of evolution. Because of these simplifications, one has to ensure that the results obtained by the numerical way are in agreement with the physical behaviour, thus is it important to have methods to compare the experimental results and the numerical ones.

One important aspect fusion scientists are studying today is the turbulence in the scrape-off layer (SOL). The physics of this region is crucial to understand and predict the performances of future devices[1]. The aim of the present work is to compare the turbulence between various regions in the low field side SOL, mainly the X-point region (above and below) and the total low-field side. A second goal is to qualitatively understand to which extent we can infer the properties of the turbulence from the experimental measurement of the D_α Balmer emission line from Gas Puff Imaging on TCV.

2 Theory

The simulation of the SOL region of the TCV is performed by the Global Braginskii Solver code (GBS) which is a numerical implementation of the Braginskii equations in the drift limit, able to perform three-dimensional simulation of the plasma in tokamak devices. The details of its implementation,

its physical assumptions and its equations are detailed in Ref. [2]. The simulation is done over a grid of $154 \times 303 \times 64$ points in the x, y poloidal plane, and in the z toroidal direction, respectively. The cartesian plane is such that when x increases, it gets closer to the wall of the low-field side. The normalizations are detailed in Ref. [2] and we state here the relevant ones for this project. The perpendicular lengths are normalized to $\rho_{s0} = c_{s0}/\Omega_{ci}$ where $c_{s0} = \sqrt{T_{e0}/m_i}$ is the reference sound speed and T_{e0} is the reference electron temperature, the perpendicular velocities are normalized to $c_{s0}\rho_{s0}/R_0$ where R_0 is the tokamak major radius, the density n is normalized to the reference density n_0 and the time is normalized to R_0/c_{s0}. In GBS, the length normalizations are fixed by setting $\rho^* = R_0/\rho_{s0}$. In our case, we have $R_0 = 0.9\,\mathrm{m}$.

The turbulence we are describing here are blobs. Blobs are regions of enhanced density in the plasma. When appearing in a tokamak, the curvature and $\nabla\mathbf{B}$ forces will result in radial motion of this blob in the direction of the wall. A basic blob model and a more detailed discussion can be found in Ref. [3]. Let $n(x, y, t)$ be the plasma density at a given position (x, y) in a fixed poloidal plane z and at a given time t. A point is considered to be part of a blob if:

$$n(x, y, t) > \bar{n}(x, y) + \alpha n_{rms}(x, y) \tag{1}$$

where $\bar{n}$ and n_{rms} are the local toroidally and time-averaged density and its standard deviation, respectively, and α is a threshold which controls the criterion to accept a blob. All the neighbouring points of the grid that meet the criterion eq. (1) are part of the same blob. For a given poloidal plane, the density from the simulation will be investigated to detect blobs. From a frame to the next one, two blobs will be considered to be the same if they share at least 10% of their area. With this criterion, we can detect if a blob splits in two or more blobs, if multiple blobs merge together and if a blob disappears.

In this project we want to analyse the size and velocity properties of the blobs in various regions of the SOL and in different experimental configurations. In particular, we want to characterise the radial and poloidal velocity in the field-aligned coordinates (r, χ), which are detailed in Ref. [2]. Since the numerical simulations are performed over a cartesian grid, it is easier to extract and manipulatesthe quantities of interest in cartesian coordinates and then transform the result into the field-aligned coordinates. Hereafter we will explain the theoretical concepts and methods needed for our analysis. The results will be presented in Sec. 3 and a discussion about these will follow in Sec. 4.

2.1 Temporal fluctuation of density

First, we will search for intervals of χ-coordinate of interest in the SOL by monitoring the regions where there are high temporal fluctuations of density, because this is an indication of the presence of blobs. The temporal fluctuation of density is defined by:

$$\delta n_\chi(t) = \bar{n}_\chi(t) - \langle \bar{n}_\chi \rangle \tag{2}$$

where $\bar{n}_\chi(t)$ is the space averaged density (average over the whole radius r, a given χ-coordinate interval and the whole toroidal direction z) and $\langle \bar{n}_\chi \rangle$ is its time average, over the whole simulation period. In practice, we load the result of a simulation (a diverted configuration Lower Single Null in our case, see Fig. 1) and extract the quantity of interest, which is in our case the density, over the whole space and the whole period of simulation. The result files are heavy and exceed the computer's memory if one simply loads them over the whole time period. Instead one can load the result files on a smaller number of time steps, extract the observable, then repeat and at the end concatenate the data from each smaller

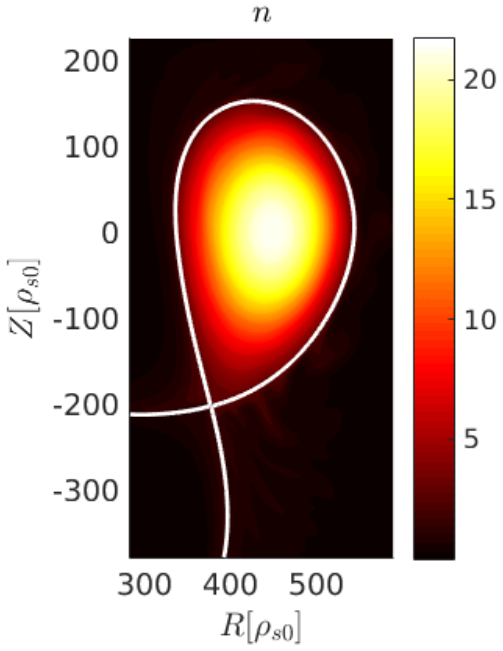

Figure 1: Plasma density in a poloidal plane in a diverted configuration Lower Single Null. The white curve is the separatix.

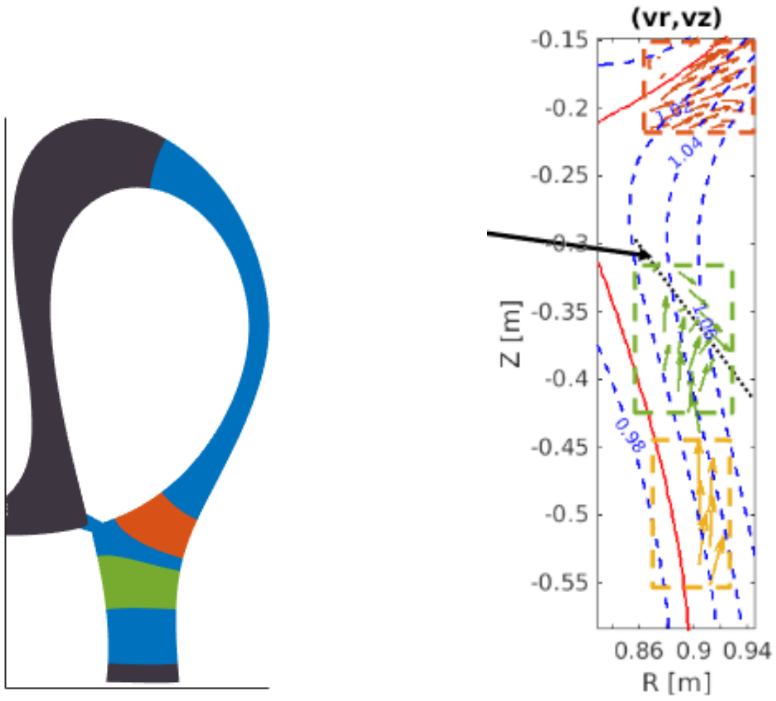

(a) (b)

Figure 2: Regions of the scrape-off layer in a poloidal plane in which we will investigate the blobs. For the numerical simulations (a), the regions are: the low-filed side (in blue), above the X-point (in orange) and below the X-point (in green); and for the experimental data (b) the regions are: above the X-point(in red), below the X-point (in green) and at the very bottom of the SOL (in yellow).

time period. The density now loaded is in cartesian coordinates and so we convert it in field-aligned coordinates. Finally we compute the space average, the time average and then take the difference between the two to have the fluctuation of density $\delta n_\chi(t)$, and we repeat the same process for ~ 40 χ-coordinate intervals.

2.2 Blobs analysis

After observing fluctuations in density, the key elements we need to observe, analyse and understand are the density blobs. Unfortunately, it is very difficult experimentally to directly observe the density in the plasma and what we do instead is to perform indirect observations of the density. One candidate for this is to observe the D_α line of emission of the Balmer series with a technique called gas puff imaging (GPI), which is explained in full details in Ref. [4] and we summarize here the relevant information. The D_α line of the Balmer series is used because its rate of emission is approximately related to the density by:

$$D_\alpha = n n_n r_\alpha(n, T_e) \tag{3}$$

where n is the electron density, n_n is the atomic neutral density and $r_\alpha(n, t_e)$ is the emission rate coefficient of the D_α line, which depends on the electron density and temperature. Since most of these emitted photons will leave the plasma without interacting with it because it is optically thin in typical tokamak conditions, these emission lines can be observed by fast cameras with high temporal and spatial resolution. From eq. (3) we see that the rate of emission is proportional to the atomic neutral density. Therefore, to increase the emission rate, we inject neutral gas in the region where we want to observe the blobs so that we can better observe the behaviour of the plasma.

However, we have to keep in mind that the quantity of interest is still the density, in particular the regions of enhanced density. So we want to compare to which extent we can infer the density of the plasma from the measurement of the D_α lines of emission from GPI. To do so we will proceed to a series of comparisons between configurations that go from blobs of density obtained by numerical simulation

to experimental data measured using GPI. In particular, with simulation results we will compare the average (over the number of blobs) radial and poloidal velocities of the blobs v_r and v_χ as a function of the radial coordinate r, as well as the histogram of the area of the blobs A_b in three regions of the SOL: above the X-point, below the X-point and over the whole low-field side; and experimental data have been measured in the following regions: above the X-point, below the X-point and at the very bottom of the SOL, see Fig. 2. This analysis is performed over the whole simulation time but only on one poloidal plane (the first one).

We will first investigate to which extent does adding gas puff affect the blobs. To do so, we will compare the density blobs velocities and the D_α blobs velocities between a simulation without gas puff and a simulation with gas puff. The D_α quantity is numerically implemented using eq. (3) and the criterion for a D_α blob is the same as the one that is used for the density, i.e. eq. (1), but by replacing n by D_α. Secondly, using the same numerical results, we will examine to what degree can one infer the velocities of the density blobs from the D_α blobs. Finally, we will compare how the D_α blobs from the simulation with gass puff resemble the experimental blobs measured by GPI. To perform these analysis on simulation results, there has to be enough detected blobs. If too few are detected because the simulation is not long enough, one can decrease a little bit the blob threshold α appearing in eq. (1). For the simulation without gas puff, we used $\alpha = 2.5$ and for the simulation with gas puff, we used $\alpha = 2$.

3 Results

3.1 Temporal fluctuation of density

Fig. 3 presents the numerical results of the temporal density fluctuation as explained in Sec. 2.1. The fluctuations with highest amplitude are located in the interval $\chi \in (\sim 180, \sim 340)$ a.u., i.e. the low-field side up to the X-point.

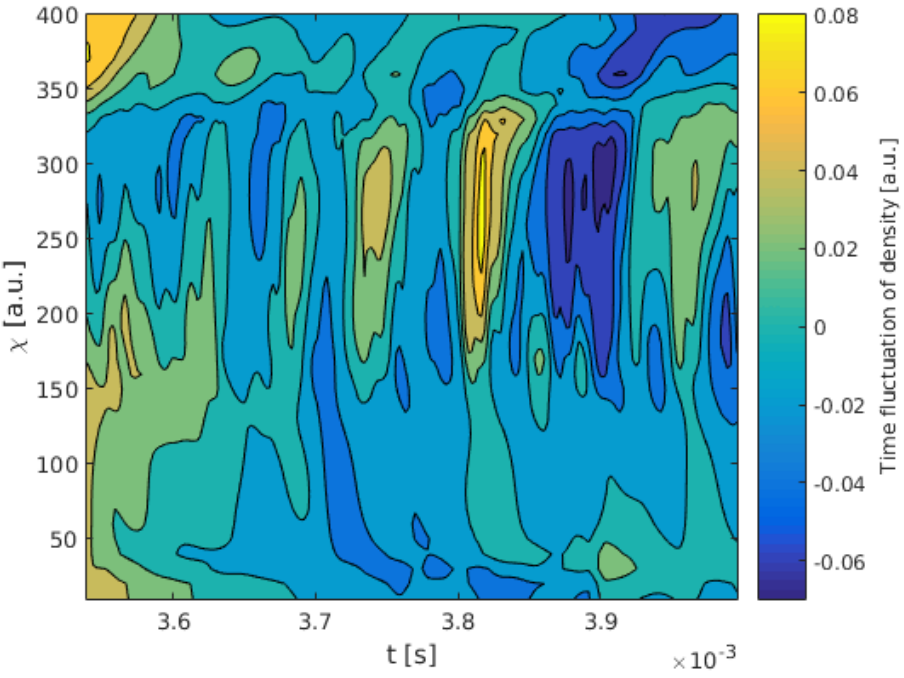

Figure 3: Numerical result of temporal density fluctuation as defined in eq. (2) for each value of the χ-coordinate. The fluctuations with highest amplitude are located within $\chi \in (\sim 180, \sim 340)$ a.u. which corresponds to the low-field side up to the X-point.

3.2 Blobs analysis

Fig. 4 presents the average density and D_α blobs velocities v_r, v_χ vs the radial coordinate r from a numerical simulation **without gas puff**.

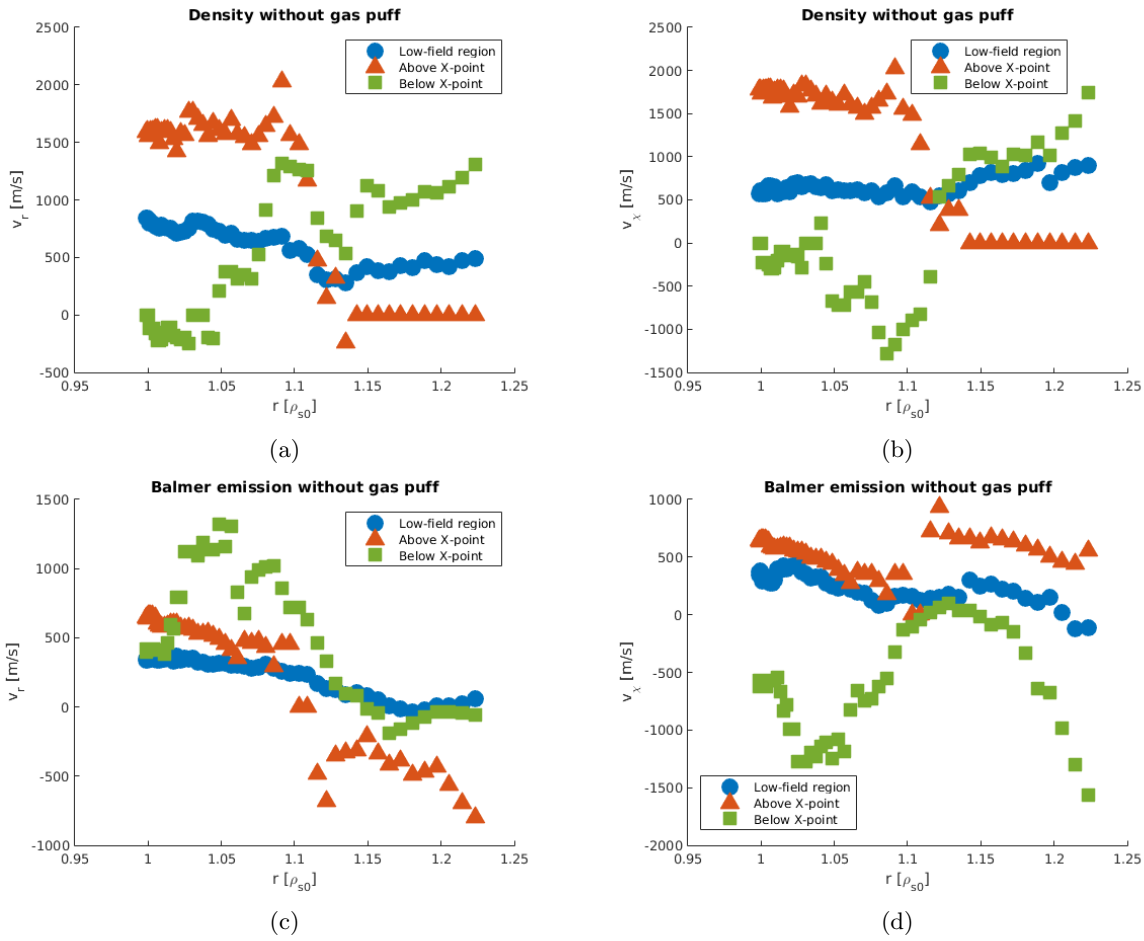

Figure 4: Average blobs velocities v_r, v_χ vs the radial coordinate r in three regions of the SOL: the low-field side (in blue), above the X-point (in orange) and below the X-point (in green) as showed in Fig. 2 from a numerical simulation **without gas puff**. Radial velocity v_r of the density blobs in (a), poloidal velocity v_χ of the density blobs in (b), radial velocity v_r of the D_α blobs in (c), poloidal velocity v_χ of the D_α blobs in (d).

Fig. 5 presents the average density and D_α blobs velocities v_r, v_χ vs the radial coordinate r from a numerical simulation **with gas puff**.

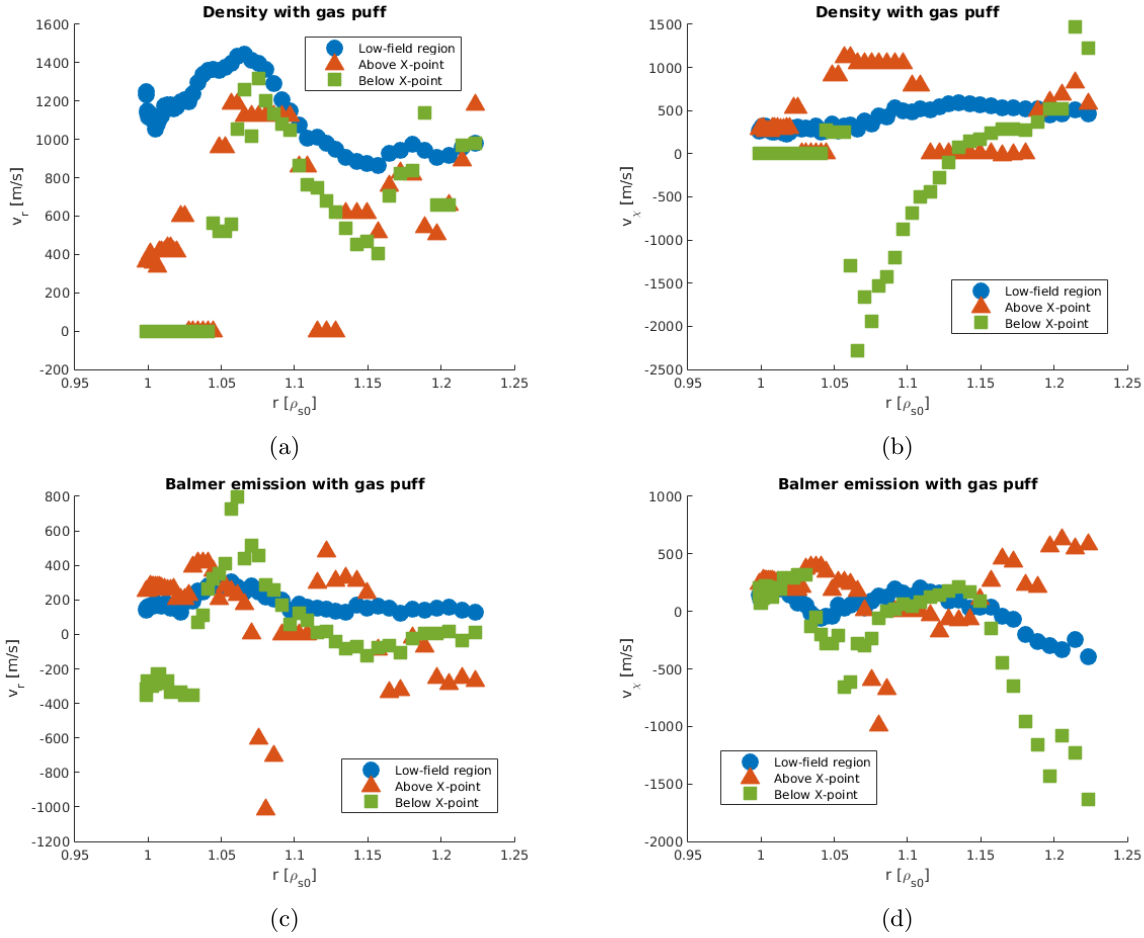

Figure 5: Average blobs velocities v_r, v_χ vs the radial coordinate r in three regions of the SOL: the low-field side (in blue), above the X-point (in orange) and below the X-point (in green) as showed in Fig. 2 from a numerical simulation **with gas puff**. Radial velocity v_r of the density blobs in (a), poloidal velocity v_χ of the density blobs in (b), radial velocity v_r of the D_α blobs in (c), poloidal velocity v_χ of the D_α blobs in (d).

Fig. 6 shows the average D_α blobs velocities v_r, v_χ vs the radial coordinate r from a numerical simulation with gas puff and real measurements data taken with GPI. The measurements have been done over $r \in (0.985, 1.070)\,\rho_{s0}$ therefore the x-axis of the numerical results has been rescaled to allow the comparison between the two.

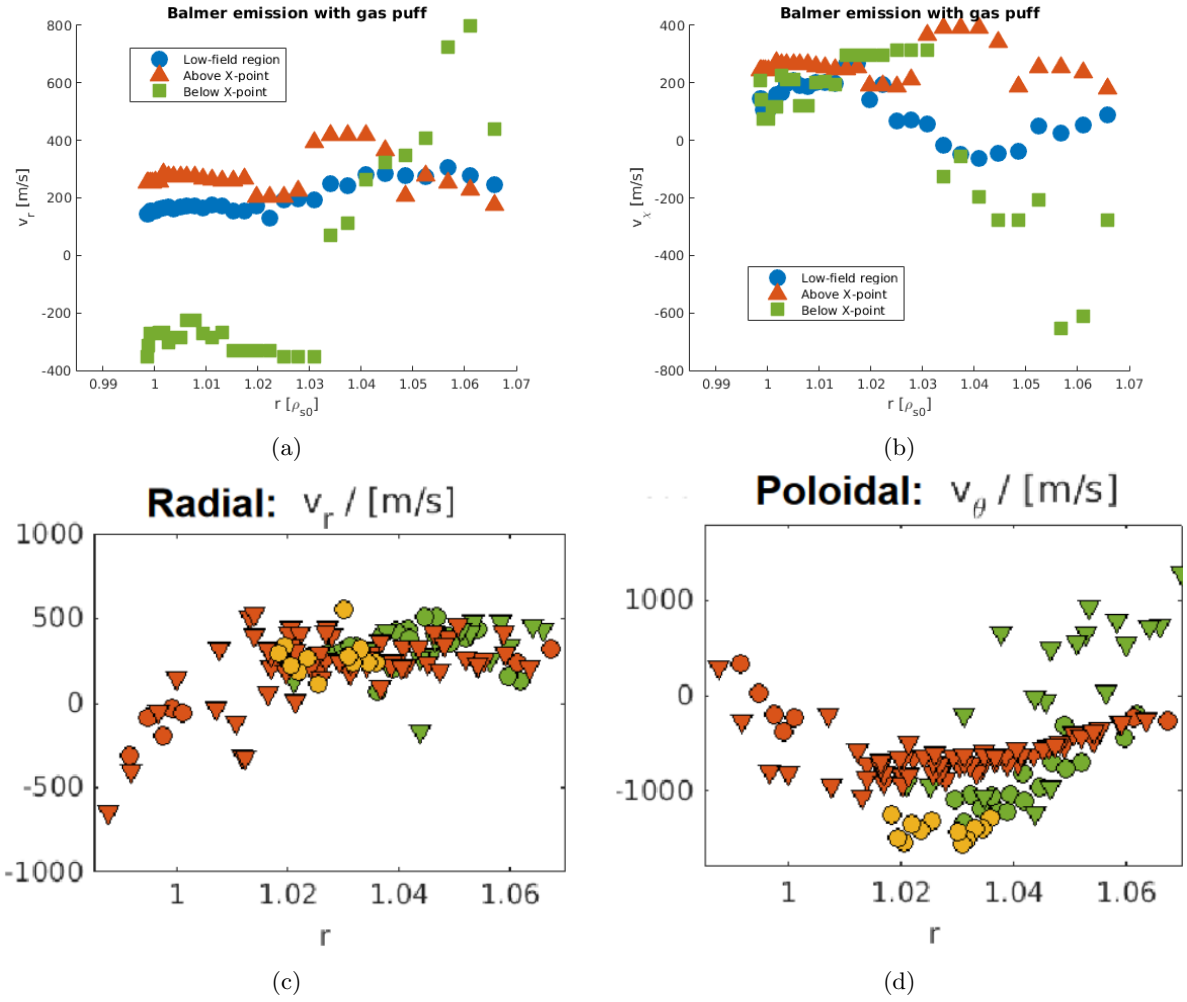

Figure 6: Comparison of the average blobs velocities v_r, v_χ vs the redial coordinate r between a numerical simulation with gas puff and experimental data obtained using GPI. The regions of the SOL where the blobs in the simulation are investigated are: the low-field side (in blue), above the X-point (in orange) and below the X-point (in green) as shown in Fig. 2a; and the regions of the SOL where the blobs are measured are: above the X-point(in red), below the X-point (in green) and at the very bottom of the SOL (in yellow) as shown in Fig. 2b. Radial velocity v_r of the simulated D_α blobs in (a), poloidal velocity v_χ of the simulated D_α blobs in (b), radial velocity v_r of the GPI D_α blobs in (c), poloidal velocity v_χ of the GPI D_α blobs in (d). The sign convention of the poloidal velocity in the simulation is inverted compared to the poloidal velocity from experimental data, therefore one has to keep in mind that one has to take a minus sign when comparing the two. The plots of the experimental data are from Ref. [5] and have been adapted for the present document.

Fig. 7 presents the histograms of the area A_b of the density and D_α blobs in simulations without and with gas puff.

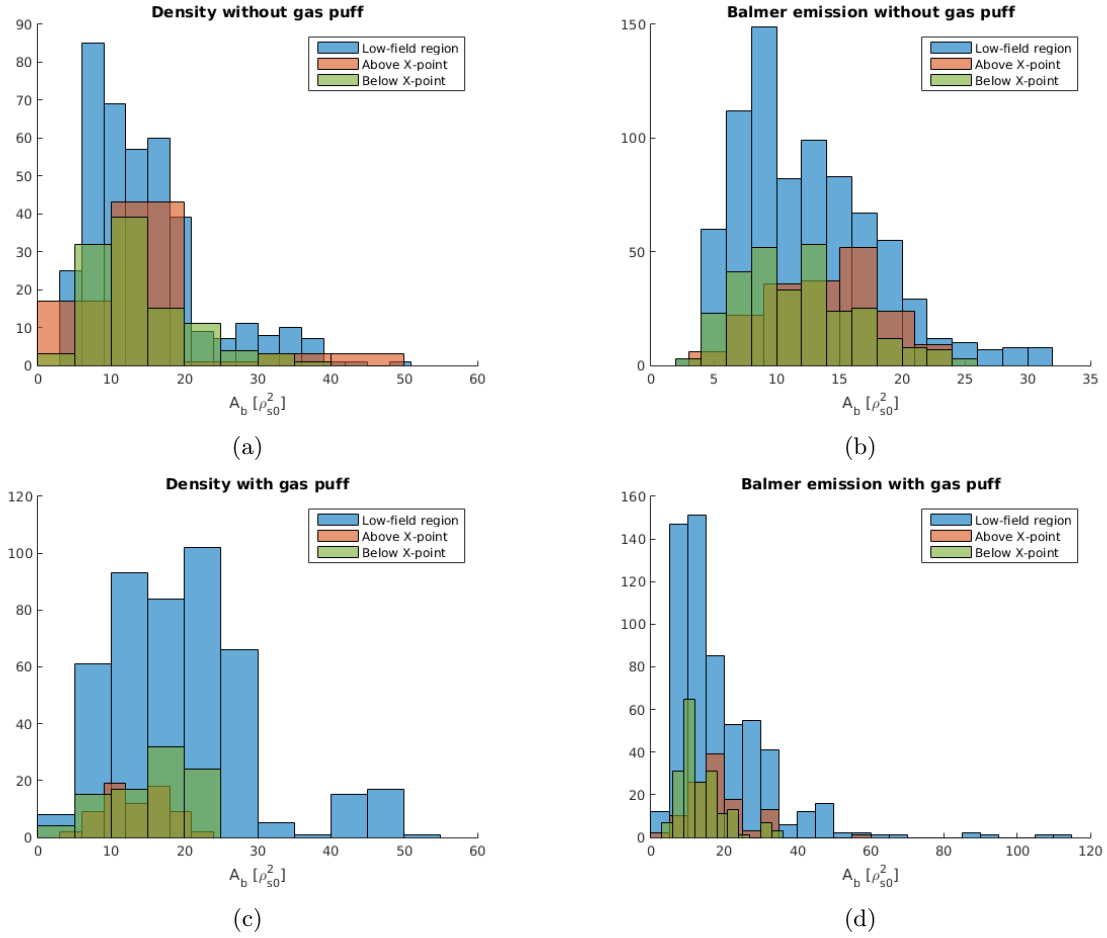

Figure 7: Histogram of the blobs area A_b from the numerical simulations in three regions of the SOL: the low-field side (in blue), above the X-point (in orange) and below the X-point (in green) as shown in Fig. 2. Histogram of the density blobs size without gas puff in (a), histogram of the D_α blobs size without gas puff in (b), histogram of the density blobs size with gas puff in (c) and histogram of the D_α blobs size with gas puff in (d).

4 Discussion

4.1 Temporal fluctuation of density

We can see on Fig. 3 that there are fluctuations at any value of χ but the highest amplitudes of fluctuations are located in the low-field side, especially from the top of the SOL up to the X-point. This confirms that this is a region of interest regarding the blobs.

4.2 Blobs analysis

One should be very careful when analysing these plots because our brain easily recognises patterns even when there are not and since here this is only a qualitative comparison (and not a quantitative one), we are particularly prone to these biases.

From Fig. 4 we first see that in the same simulation without gas puff, the curves for density blobs and D_α blobs are not always similar. The radial and poloidal velocities over the whole low-field side is approximately flat for both, with order of magnitude $\sim 10^2$ m/s, but the comparison is not the same when comparing the density blobs and the D_α blobs in the region above the X-point and below the X-point. The orange and green points do not seem to share a similar behaviour when observing the density blobs and the D_α blobs, for both the radial and the poloidal velocity. In the region above the X-point (orange curves), the average radial and poloidal velocities of density blobs are flat for $r \in (1.15, 1.25)\,\rho_{s0}$, indicating that we did not observe blobs in this region, whereas in the same region and same interval for r, we did observe D_α blobs. This indicates that the behaviour of the density blobs and the D_α blobs are very different in these regions. One cause of these differences could be that the time period of the simulation was too short, and then too few blobs have been detected to extract statistical information from it.

The observation is broadly similar in the simulation with gas puff (Fig. 5), again we could be tempted to say that there are some similar behaviour between the density blobs curves and the D_α blobs curves, but it could just as easily be random patterns that our brain sees as similarities.

When comparing the behaviour without and with gas puff (Fig. 4 and 5) we see not so many similarities, except the green curve that seems to have similar peaks but the other curves do not share any obvious similar behaviours. Again, we suspect that this is because the duration of the simulations was not big enough and we have not enough data to infer the average behaviour in these regions. Hence, we should not give great confidence in these results, we expect that repeated with another simulations, for a longer time, the results would be significantly different.

Even though the previous analysis did not conclude, the comparison between the simulation results and the experimental measurements , Fig. 6, looks more accurate. Indeed, for $r \in (1, 1.07)\,\rho_{s0}$ the radial velocity v_r above the X-point (orange/red curves) is flat and with order of magnitude $\sim 10^2\,$m/s for both the simulation and the measurement. This is less obvious below the X-point since there are measurements that are missing in the range $r < 1.02$, but for $r > 1.02$ we have a radial velocity with the same order of magnitude $\sim 10^2$ m/s. It appears that in the simulation this velocity increases with the radius, a behaviour partially observed by the experimental measurements but these measurements have a low precision hence we cannot compare in more detail this curve. Regarding the poloidal velocity v_χ, we recall that the direction do not follow the same convention between the simulation and the experiment, and one has to take the data with opposite sign to compare the two. With this remark in mind, we see that the numerical poloidal velocity above the X-point resemble the experimental data in the sense that it is approximately flat for $r > 1\,\rho_{s0}$ but here the amplitude seems different, around 200 m/s for the simulation and around 1000 m/s for the experimental data. In the region below the X-point (in green), we see the poloidal velocity decreasing from a positive to a negative value (or opposed sign depending on the convention) but the multiplicative factor is different from the simulation results and the experimental measurements.

We clearly see some similar behaviours when comparing the simulation data and the experimental measurements of the radial and poloidal velocities, and this tends to show that our numerical analysis has been done correctly. However, the fact that the results are so different when adding the gas puff or not, or looking at density blobs or D_α blobs, this makes us doubt the veracity of our analysis. Our hypothesis to explain these differences is that the number of simulation steps used to perform these analysis was too small and the results here do not accurately represent the average behaviour.

On Fig. 7 we see that in each configuration (density and D_α blobs, without and with gas puff, in the whole low-field side, above the X-point and below the X-point) the typical blob has an area close to $\sim 10\,\rho_{s0}^2$ and the histogram has a width $\sim 20\,\rho_{s0}^2$. This measure of the area is a first indication about the shape of the blobs but it does not allow us to discuss in more detail if the blobs are elongated, in which direction, if their shape changes when they move, etc.

5 Conclusion

Our analysis of the temporal fluctuations of the density in different lines of sight represented by a different χ-coordinate clearly indicates that there are turbulence in the low-field side. But these turbulence have been difficult to analyse. We aimed to determine their radial and poloidal velocities as a function of the radial coordinate r but the results were very different depending on the configuration: a simulation without or with gas puff, and observe the blobs of density or the blobs of D_α, a Balmer emission line. More generally, the aim was to determine to which extent one can infer from the measurement of the D_α blobs the properties of the density blobs. Due to these differences between the configuration, we are tempted to claim that we cannot infer the radial and poloidal velocities of the blobs from the measurements of the D_α emissions. However, this claim is based on qualitative analysis only and there could be some better inference strategies to recover the ground truth density from the Balmer emission. Moreover, our analysis suffers from a lack of data which means that we have not been able to highlight the average behaviour of the curves.

We could also think that the differences of the trends between the different configurations are due to some errors in the codes used to generate these results. Fortunately, we tend to refute this hypothesis because when comparing between the simulation results and the experimental measurements taken with GPI, there were promising resemblances.

To continue the analysis of the turbulence in more depth, one could first do the same analysis done here but with a larger number of data, i.e. over a larger number of time steps, and also with more simulations to ensure that the results are reflecting the average behaviour. One could also describe in more details the properties of the blobs in this configuration, something similar to what has been done in Ref. [6], i.e. some characterization of the blobs size and shape, their velocity etc.

References

[1] P. Ricci, "Simulation of the scrape-off layer region of tokamak devices," *Journal of Plasma Physics*, vol. 81, no. 2, p. 435810202, 2015.

[2] M. Giacomin, P. Ricci, A. Coroado, G. Fourestey, D. Galassi, E. Lanti, D. Mancini, N. Richart, and N. Varini, "The GBS code for the self-consistent simulation of plasma turbulence and kinetic neutral dynamics in the tokamak boundary." Preprint submitted to Computer Physics Communications, May 2021.

[3] D. A. D'Ippolito, J. R. Myra, and S. J. Zweben, "Convective transport by intermittent blob-filaments: Comparison of theory and experiment," *Physics of Plasmas*, vol. 18, p. 060501, June 2011.

[4] C. Wersal and P. Ricci, "Impact of neutral density fluctuations on gas puff imaging diagnostics," *Nuclear Fusion*, vol. 57, p. 116018, aug 2017.

[5] C. Wüthrich, C. Theiler, N. Offeddu, D. Galassi, D. S. Oliveira, B. P. Duval, O. Février, T. Golfinopoulos, W. Han, C. L. Tsui, and the TCV team, "X-point and divertor filament dynamics from gas puff imaging on TCV." Poster for the 47th Conference on Plasma Physics, European Physical Society.

[6] F. Nespoli, I. Furno, B. Labit, P. Ricci, F. Avino, F. D. Halpern, F. Musil, and F. Riva, "Blob properties in full-turbulence simulations of the TCV scrape-off layer," *Plasma Physics and Controlled Fusion*, vol. 59, p. 055009, May 2017.